

Multiple resonances in microdisk lasers of π -conjugated polymers

R. C. Polson and Z. V. Vardeny^{a)}

Department of Physics, University of Utah, Salt Lake City, Utah 84112

D. A. Chinn

Sandia National Laboratories, Livermore, California 94551

(Received 9 April 2002; accepted for publication 25 June 2002)

We have fabricated microdisk lasers from π -conjugated polymers that show multiline emission spectrum upon optical excitation. Using Fourier transform analysis, each emission line is assigned integer to an interger Bessel function that helps to estimate the field distribution inside the photoexcited polymer microdisk. We found that the microdisk can sustain two different laser modes with different, though complementary, field distributions and that the index of refraction decreases with increasing excitation intensity. © 2002 American Institute of Physics.

[DOI: 10.1063/1.1502002]

Microdisks are small, photolithographically defined circular resonance structures with an inherently high optical quality factor, Q . One use of such structures is to fabricate microlasers based on high luminiscent materials.¹⁻⁴ Other uses are to investigate material optical properties such as laser threshold,⁵ spontaneous emission efficiency,⁶ and its time dynamics.⁷ Microdisks of π -conjugated polymers have been reported previously for an active medium such as a substituted poly (phenyl vinylene), namely poly(dioctyloxy) phenylene vinylene or DOO-PPV. An 8 μm diameter microdisk laser demonstrated an emission spectrum consisting of only one logitudinal mode.⁸ In this letter we show that the investigation of larger diameter π -conjugated polymer microdisks has led to some unexpected physical effects such as different resonant laser modes in the cavity and a decrease of the polymer index of refraction at higher excitation intensities.

Photolithographic fabrication and reactive ion etching techniques borrowed from semiconductor manufacturing allow the fabrication of microdisks from films of DOO-PPV. A 1 μm film of the polymer is spin cast onto a glass substrate. Photoresist is then spun on top of the polymer and circles are patterned into the resist. The polymer is then etched in a plasma and the remaining resist is removed. The resulting polymer microdisks are then optically excited at 532 nm with 100 ps pulses of the second harmonic of a Nd:YAG regenerative amplifier. The microdisk devices are photoexcited in vacuum to avoid photodegradation. The laser emission is collected with a 1 mm diameter fiber optic placed several millimeters from the device. The emission is sent through a $1/2m$ spectrometer, detected with a charge coupled device, CCD, and recored on a personal computer. The overall spectral resolution of the collection setup is 0.02 nm. The polymer microdisk investigated here has a diameter of 55 μm and a thickness of 1 μm , for an active volume of 2400 μm^3 or $2.4 \times 10^{-9} \text{ cm}^3$.

Figure 1(a) is a SEM image of the polymer microdisk profile taken by tilting the substrate an angle of 40 degrees. The wall profile shows a smooth face, which means there is

little scattering due to surface roughness. These physical characteristics define a microcavity which allows for optical feedback and laser emission. Figure 1(b) is the top view of the microdisk showing the smooth boundary with a surface roughness on the order of 300 nm. The smooth circular boundary allows for total internal reflection to confine the emission.

Figure 2(a) is the emission spectrum from the 55 μm diameter microdisk laser measured above the threshold intensity. There are many well spaced and narrow emission lines. A closer examination of the spectrum reveals two series of modes, one series, a has a larger amplitude than the other. For the larger intensity peaks, the spacing, $\Delta\lambda_a$ for the

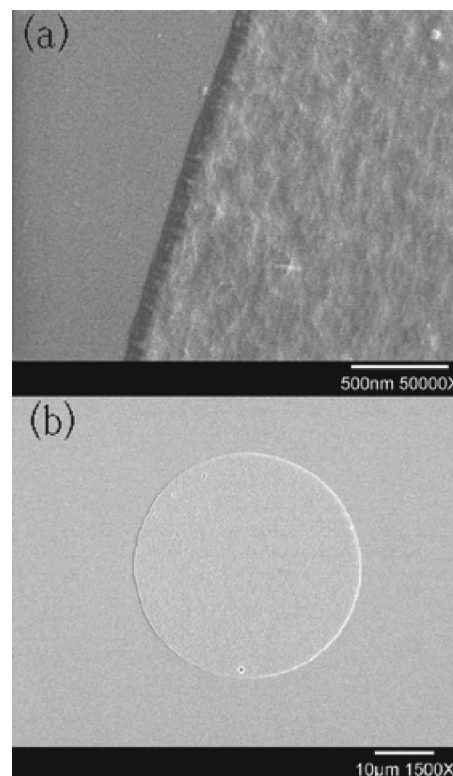


FIG. 1. Scanning electron microscope image of the microdisk; (a) is the wall profile and (b) is the top view.

^{a)}Electronic mail: val@physics.utah.edu

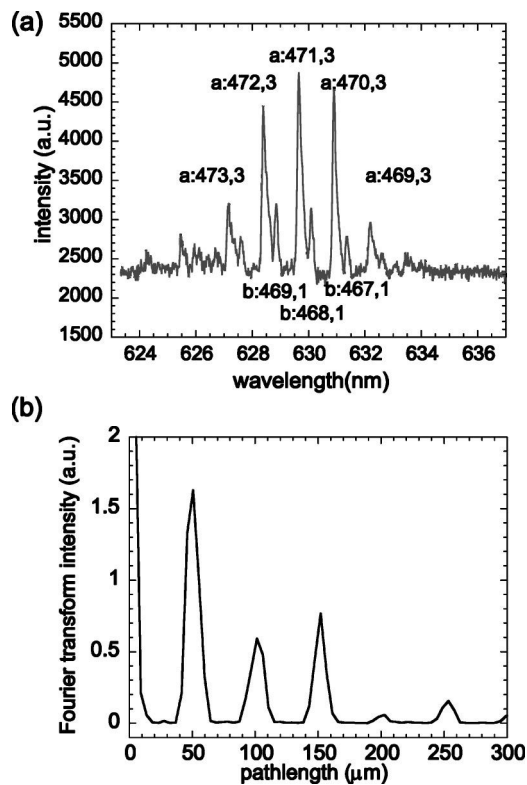


FIG. 2. (a) DOO-PPV microdisk laser emission spectrum above excitation threshold intensity; (b) Fourier transform of the emission spectrum shown in (a).

modes averages 1.27 nm, while for the smaller peaks the spacing $\Delta\lambda_b$ averages to 1.31 nm. The equation for mode spacing of a Fabry-Perot cavity can be used where the roundtrip distance $2L$ is replaced by the microdisk circumference πD ; the expected mode spacing is then $\Delta\lambda = \lambda^2/n\pi D$, where n is the index of refraction and D is the disk diameter.⁹ The mode spacing values would suggest that the product of index of refraction and diameter, nD is different for the two mode series.

The very narrow emission lines indicate that the cavity quality factor, Q is high, on the order of 3000, and only little emission escapes during each cycle. The cylindrical geometry of the disk allows the wave equation to be separated into different analytic functions in each of the r and θ directions¹⁰ with the radial direction consisting of Bessel functions. Since the Q value is high, an approximation can be made that the fields go to zero at the polymer air interface. For the field to be zero everywhere along the interface, the argument of the integer Bessel function, $J_s(kr)$ must be zero at the boundary:

$$J_s(2\pi nR/\lambda) = 0, \quad (1)$$

where R is the disk radius. Bessel functions have many zeros, so this condition can be written as

$$X_{st} = (2\pi nR/\lambda), \quad (2)$$

where X_{st} indexes the t th zero of Bessel function of order s .

In order to describe all the modes, the product of nR must be known to several decimal places. An accurate value of nR comes directly from the Fourier transform of the emission spectrum.⁹ Figure 2(b) is the Fourier transform of the emission spectrum 2(a). If the units of the emission spectrum are measured in wave vector ($k = 2\pi/\lambda$) then the units of the

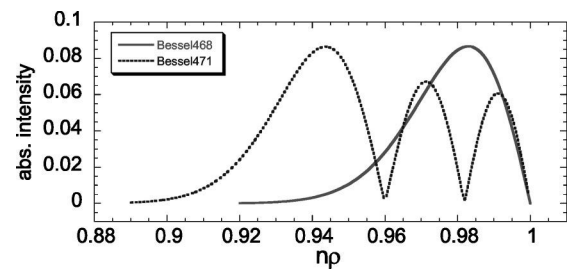


FIG. 3. Field distribution for Bessel functions $s_{0,a}=471$ and $s_{0,b}=468$ that describe the two laser mode series (a) and (b) of the polymer microdisk. The two Bessel functions are normalized so that the first zero of $s_{0,b}=468$ and the third zero of $s_{0,a}=471$ is at the boundary, respectively.

Fourier transform are length.¹¹ In Fig. 2(b) we see a single series of well spaced peaks. The Fourier transform gives peaks at nR at $50.7 \mu\text{m}$. The physical disk diameter, $D = 2R$ is $55 \mu\text{m}$ and from the measured value of nR gives 1.84 as the effective index of refraction. This value indicates that the fields of the modes are entirely contained within the polymer disk since the index of refraction of the DOO-PPV polymer is 1.8, which we measured by ellipsometry on an unetched polymer film.

An attempt is shown to fit the strongest peak in the emission spectrum at $\lambda_{0,a} = 629.65 \text{ nm}$. The starting Bessel index s_0 is how many wavelengths can fit around the perimeter. For the polymer disk we get $s_0 = 503$. The first zero of Bessel function 503 occurs at 517.89, which when using Eq. (2) with $nR = 50.7 \mu\text{m}$ from the Fourier transform gives an expected wavelength of $\lambda_{0,a} = 615.01 \text{ nm}$, in disagreement with the data. Investigation of Bessel functions with the first zero at the polymer air interface near s_0 reveals that $s = 491$ fits reasonably well with an expected wavelength $\lambda_{0,a} = 629.75 \text{ nm}$, which is a difference of 0.1 nm from the measured value. In this laser mode, the index of refraction versus radius $n(r)$ has a single discontinuity at the edge of the disk. It may be then that the field goes to zero not at the first zero of a Bessel function, but at a higher order zero. Attempting to use a higher zero yields an even better match. With the third zero of Bessel function $s_0 = 471$, the predicted wavelength value $\lambda_{0,a} = 629.67 \text{ nm}$ for the main emission peak. The difference of 0.02 nm is within the system resolution. Neighboring emission peaks correspond to successive integer values of Bessel functions. The entire series of main peaks can thus be fit with a series of Bessel functions as seen in Fig. 2(a). The greatest discrepancy is just 0.08 nm for the series of seven peaks described by a series of Bessel functions $468 < s < 474$ and the product of $nR = 50.7 \mu\text{m}$. We note that there are no adjustable parameters in this fit.

The minor peaks in the emission spectrum of Fig. 2(a), the b series, have yet to be considered. Neither the first nor the third zeros of any Bessel functions accurately describe these peaks. Some sort of echo effect is unlikely since they have a different spacing than the main peaks. The spacing, $\Delta\lambda_b$ of these peaks is larger than $\Delta\lambda_a$ indicating that the product nD is smaller for this laser mode. The Fourier transform does not seem to show a second cavity, only singular harmonics are present. The spacing of the minor peaks, $\Delta\lambda_b$, is about 3% larger than the major peaks; the spacing of points in the Fourier transform is $4.6 \mu\text{m}$, which is roughly 3% of the product of nD , or $101.4 \mu\text{m}$. The next point below

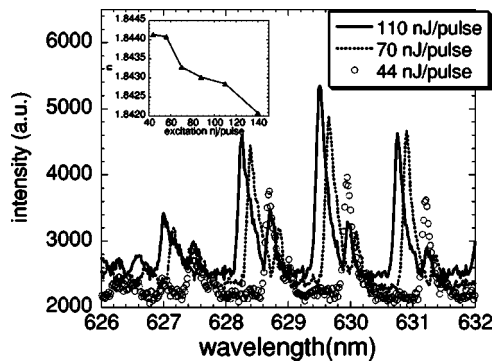


FIG. 4. Microdisk laser emission at several intensities. The inset shows the effective refractive index vs intensity, which was obtained from the Fourier transform of the emission spectra.

101.4 μm in the Fourier transform occurs at 96.8 μm in Fig. 2(b) and we will then use this value for nD to fit the minor peaks. The same fitting procedure used to fit the major peaks will be used to fit the most intense minor peak occurring $\lambda_{0,b} = 630.09$ nm. The first zero of Bessel function $s = 468$ gives a wavelength $\phi\lambda_{0,b} = 630.06$. The neighboring minor peaks fit nicely in a series with nD 96.8 μm . Higher zeros do not seem to fit well. Again, the series of six minor peaks is described with no adjustable parameters with $467 < s < 472$.

Insight as to why the same disk can support these two laser mode series is provided by plotting the field distributions. The absolute value of Bessel functions $s_{0,a} = 471$ and $s_{0,b} = 468$ are plotted in Fig. 3. In this figure Bessel function 471 has been scaled so that the third zero occurs at the disk radius and Bessel function 468 has the first zero scaled at the disk radius. We see that the field distribution for the major peaks (a) penetrates further into the interior of the disk and extends through more gain medium. The highest intensity for either normalization occurs just before the first zero. It is now apparent that the field distribution for the function with three maxima $s_{0,a}$ has gaps where the field intensity is close to zero. If another field distribution can occur in the physical space where the first field has minima, then the second field may experience enough gain to lase. As plotted, the maximum of Bessel function $s_{0,b} = 468$ fits between the second and third maxima of Bessel function $s_{0,a} = 471$. The peak occurs between 0.97 and 0.99 nR .

The field from the major peaks that originates from Bessel functions with three maxima, may alter the index of refraction of the polymer in the cavity; this may explain the reason why the product nR is different for the two series of peaks. One strong indication of this possibility is observed by plotting several excitation intensities together. Figure 4

shows the emission spectra of the microdisk laser at several excitation intensities, $I_1 - I_3$. The overall pattern of the emission modes is the same, but there is a clear shift of the position of the emission spectrum. The main peak shifts from $\lambda_{0,a} = 629.94$ nm at $I_1 = 44$ nJ/pulse to $\lambda_{0,b} = 629.24$ nm at $I_3 = 140$ nJ/pulse. Assuming that this peak corresponds to Bessel function $s_{0,a} = 491$, the product of nR decreases from 101.43 μm at I_1 to 101.31 μm at I_3 . The microdisk diameter should increase due to heating making nR larger at higher excitation intensities. We thus conclude that the main effect is the change in the polymer index of refraction with I .

At higher intensities the polymer's index of refraction decreases. The inset of Fig. 4 shows the change of n with excitation intensity by solving Eq. (2) for n given the observed emission wavelength and assuming a constant value for R . If the index change is due to the field intensity, then the average index of refraction between the second and third maxima of the main peak's field would be less than the interior of the polymer disk. The regions with a lower index of refraction between the second and third maxima is where the Bessel functions with one maxima occurs and this explains why the peaks correspond to a value of nR that is slightly less than the rest of the polymer disk.

In conclusion, the Fourier transform of polymer microdisk emission spectrum has allowed assignment of the laser emission lines to integer Bessel functions. The same disk can support two different field patterns, which leads to the appearance of a major and minor series of peaks in the laser emission spectrum. The index of refraction of the polymer has been shown to be intensity dependent.

At the University of Utah we acknowledge financial support from NSF Grant No. DMR02-02790, DOE Grant No. FG-03-93ER45490, and a Grant in Aid from Sandia (DOE).

- ¹S. L. McCall, A. F. J. Levi, R. E. Slusher, S. J. Pearton, and R. A. Logan, *Appl. Phys. Lett.* **60**, 289 (1992).
- ²D. Y. Chu, M. K. Chin, N. J. Sauer, Z. Xu, T. Y. Chang, and S. T. Ho, *IEEE Photonics Technol. Lett.* **5**, 1353 (1993).
- ³M. Kuwata-Gonokami, R. H. Jordan, A. Dodabalapur, H. E. Katx, M. L. Schilling, R. E. Slusher, and S. Ozawa, *Opt. Lett.* **20**, 2093 (1995).
- ⁴R. A. Mair, K. C. Zeng, and J. Y. Lin, *Appl. Phys. Lett.* **72**, 1530 (1998).
- ⁵R. E. Slusher, A. F. J. Levi, and U. Mohideen, *Appl. Phys. Lett.* **63**, 1310 (1993).
- ⁶M. K. Chin, D. Y. Chu, and S. T. Ho, *J. Appl. Phys.* **75**, 3302 (1994).
- ⁷K. J. Luo, J. Y. Xu, and H. Cao, *Appl. Phys. Lett.* **78**, 3397 (2001).
- ⁸S. V. Frolov, A. Fujii, D. Chinn, Z. V. Vardeny, K. Yoshino, and R. V. Gregory, *Appl. Phys. Lett.* **72**, 2811 (1998).
- ⁹R. C. Polson, G. Levina, and Z. V. Vardeny, *Appl. Phys. Lett.* **76**, 3858 (2000).
- ¹⁰J. D. Jackson, *Classical Electrodynamics*, 2nd ed. (Wiley, New York, 1975).
- ¹¹D. Hofstetter and R. L. Thornton, *Appl. Phys. Lett.* **72**, 404 (1998).